ORIGINAL PAPER

CrossMark

Clarifying the hydrological mechanisms and thresholds for rainfall-induced landslide: in situ monitoring of big data to unsaturated slope stability analysis

Zongji Yang[1] · Huan Cai[1,2] · Wei Shao[3] · Dong Huang[1] · Taro Uchimura[4] · Xiaoqin Lei[1] · Honglin Tian[1] · Jianping Qiao[1]

Abstract

The development of early warning systems for landslide hazards has long been a challenge because the accuracy of such systems is limited by both the complicated underlying mechanisms of landslides and the lack of in situ data. In this study, we implemented a multivariate threshold criterion that integrates in situ monitoring data and data from unsaturated hydro-mechanical analyses as an early warning system for rainfall-induced landslides in the Wenchuan earthquake region of China. The results indicate that rainfall intensity is closely correlated with the probability of landslide occurrence. Variations in matric suction and suction stress were obtained from in situ measurements and used to quantify the soil water retention curve, which presented clear hysteresis characteristics. The impacts of rainfall infiltration on slope failure in post-earthquake landslide areas under transient rainfall conditions were quantified by hydro-mechanical modelling theories. Variations in the suction stress of unsaturated soil were used to calculate the safety factor. The influence of hydrological hysteresis processes on the slope failure mechanism was analysed. Multivariate threshold criteria that include the intensity–probability (*I-P*) threshold, soil moisture and matric suction based on in situ big data and unsaturated slope stability analysis benchmarks are proposed for use in an early warning system for rainfall-induced landslides.

Keywords Rainfall-induced landslide · Hydrological mechanism · Multivariate thresholds · Early warning · Unsaturated condition · Big data

Introduction

Landslides and debris flows that occur after high-intensity rainfall represent some of the most destructive disasters in mountainous areas. It has been suggested that the development of systems for the early warning and forecasting of rainfall-induced landslides is one of the most useful non-structural countermeasures to such hazards for the prevention of landslide hazards and reduction of risks. In this context, identification of the practical and reliable rainfall thresholds that trigger landslides is essential for establishing an early warning system for such hazards. At the present time, the predominant early warning indicator methods for rainfall-induced landslides are those based on the rainfall intensity–duration (*I-D*) threshold method (Caine 1980; Wieczorek et al. 2000; Aleotti 2004; Guzzetti et al. 2008; Guo et al. 2016). These methods are based on real-time rain gauge data or precipitation predictions, and they are designed to be convenient and straight-forward methods for the predication of hazards. For example, Guo et al. (2016) proposed region-specific *I-D* thresholds based on the statistical analysis of disaster events and rainfall intensity in the Wenchuan

✉ Zongji Yang
   yzj@imde.ac.cn

1   Key Laboratory of Mountain Hazards and Surface Process, Institute of Mountain Hazards and Environment, Chinese Academy of Science, No. 9, Block 4, South Renmin Road, Chengdu, Sichuan 610041, People's Republic of China

2   University of Chinese Academy of Sciences, Beijing 100049, China

3   School of Hydrology and Water Resources, Nanjing University of Information Science and Technology, Nanjing 210044, Jiangsu, China

4   Department of Civil & Environmental Engineering, Saitama University, Saitama 338-8570, Japan

earthquake region of China. However, the lack of historical or long-term monitoring data on landslides increases the difficulty of correlating landslide occurrences with the corresponding triggering rainfall under potential future conditions (Shao et al. 2017). In addition, statistics-based rainfall thresholds generally ignore the failure mechanisms and rainfall infiltration hydrological processes of landslides; thus, single thresholds of rainfall parameters may not always be sufficiently accurate for landslide hazard predictions in practice (Sidle and Bogaard 2016; Chae et al. 2017). Therefore, analysing the relationships between landslide mechanisms and landslide triggers based on hydrological and mechanical thresholds is important, and an effective method for improving the early-warning accuracy of landslides includes a combination of hydro-mechanical mechanism analysis and real-time in situ observations (Berti and Simoni 2010; Greco et al. 2013).

Clarifying the mechanisms underlying rainfall-induced landslides represents a primary step in the development of early warning systems. It is therefore important to be able to combine in situ observations and the results of hydro-mechanical analysis with the aim to improve our understanding of the mechanisms of rainfall-triggered landslides. Physical observations are vital to improving our understanding of landslide initiation because they provide measured variables that describe the phenomenon of landslides; however, hydro-mechanical theories are essential for hazard predictions because they provide the links between the variables governing landslide processes (Godt et al. 2009; Lu and Godt 2013; Shao et al. 2016; Song et al. 2016). Many recently proposed early warning systems based on in situ landslide monitoring integrate multiple parameters, including precipitation, slope displacement and physical slope properties (Xia et al. 2014; Fan et al. 2016; Ma et al. 2016; Palis et al. 2017); however, these approaches are based on simplified statistical approaches that do not integrate unsaturated hydro-mechanical theories. Unsaturated hillslope hydrology has been widely accepted to be a significant mechanism of rainfall-induced landslides (Baum et al. 2010; Lu and Godt 2013; Yang et al. 2017); however, a multiple threshold criterion that integrates a multitude of in situ instrumental data and unsaturated hydro-mechanical methods for the early warning of rainfall-induced landslides is poorly documented in the literature.

In this study, we report our development of an integrated early warning framework that is based on multiple source criteria and which incorporates soil moisture, matric suction and rainfall intensity–probability (*I-P*) thresholds for rainfall-induced landslides by coupling instrumental monitoring big data and unsaturated hydro-mechanical analysis benchmarks. The aim of this study was to provide insights into the development of an effective and accurate early warning system for rainfall-induced mountain hazards. This type of monitoring and early warning system is urgently needed in the

Wenchuan earthquake region and in similar environments that are threatened by rainfall-induced landslides.
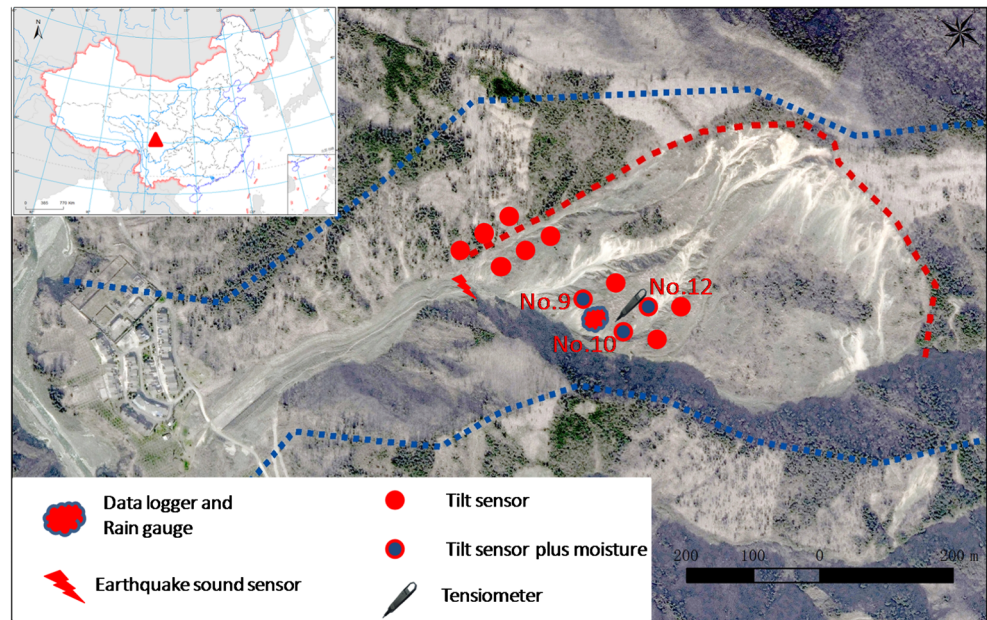
Method

The investigation reported here involved an analysis of monitoring data and simulations of the stress state and slope stability under rainfall infiltration with the aim to establish a real-time monitoring and early warning system for a natural landslide in Dujiangyan county of the Wenchuan earthquake region, China.

In situ monitoring

Integrated in situ monitoring of kinematic, physical and hydrological parameters contributes greatly to our understanding of landslide mechanisms, with the data obtained suggesting reliable thresholds for landslide early warnings. In this study, the real-time monitoring systems included instrumentation that automatically measures key state variables in landslide material. The observed data were continuously collected and sent wirelessly to facilitate remote analysis of the real-time data. These systems are effective for predicting forthcoming landslides and analysing the failure mechanisms.

In this study, the instrumented landslide is situated in the catchment area of the Baishahe river in Dujiangyan County, Chengdu, Sichuan province, which is in the meizoseismal area of the Wenchuan earthquake region (Fig. 1). The landslide was triggered by a giant earthquake whose components were mainly intensely weathered granite, andesitic and sand. In terms of soil texture, fine particles are rare in the deposit. The volume of the monitored landslide is close to one-half million stere. This landslide is located in the subtropical humid monsoon climate zone with an mean annual temperature of 16.7 °C. The mean annual precipitation exceeds 1200 mm. Rainfall is mostly concentrated in the rainy season during May to September. The landform is characterised by middle mountains with elevations ranging from 1030 to 2050 m a.s.l. at the ridges of the catchment, which retains an approximate 1-km relief along 2.5 km of gully length. The exposed strata are from the Proterozoic era and include igneous rocks, andesitic rocks and granite. These rainfall-induced shallow landslides usually evolve into an available sediment source for sequent debris flows. The landslide deposits feature a loose structure composed mainly of sand and gravel that is easily eroded by rill erosion at the free surface by rainfall and scouring flows in the hollow of the gullies at the edge of the landslide. The retrogressive slope failures caused by the effects of rainstorm and concentrated runoff have progressively enlarged the rills on the deposit, and the routing sediment in the hollow can be entrained into a debris flow driven by rainstorm events or rill erosion. Many examples of this mass transporting process in

Clarifying the hydrological mechanisms and thresholds for rainfall-induced landslide: in situ monitoring of...

2141

Wenchuan earthquake region have been recorded in the literature (Tang et al. 2009; Yang et al. 2017). As a result, in our study all sensors were carefully installed along the head of the eroded channels to capture the shallow slope failure pattern of the landslide. The slope angle of the monitoring slope along the hollow is approximately 60° on average according to a field investigation. The landslide mass was initiated and subsequently transformed into a debris flow by subsequent rain storms after the Wenchuan earthquake on August 13, 2009, July 17, 2010 and July 9, 2013 (Fig. 2). The monitored landslide and the subsequent debris flows in Yindongzi gully severely threatened the rebuilt community of Lianhe Village, Dujiangyan County, Chengdu, Sichuan province.

The real-time landslide monitoring and early warning system used in this study is shown in Fig 1; it consists of 15 pieces of equipment and the wirelessly collected data for the target landslide. In May 2014, this system, which records real-time precipitation, inclination and ground vibration as well as hydrological parameters, was established on the landslide in Yindongzi gully, Dujiangyan County ,to better define the correlations among precipitation, soil wetness and landslide activities. The rainfall data were collected using a tipping bucket rain gauge (CAWS 100; Huayun Group, Beijing, China). The soil moisture data were collected using soil moisture sensors (Decagon EC-5; ICT International, Armidale, Australia). The matric suction data were observed using a tensiometer (Tensiomark TS2; Stevens Water Monitoring Systems, Inc., Portland, OR, USA). All sensors were integrated with a wireless tilt sensor unit (Kantaro KCN-02; Chuo Kaihatsu Corporation, Tokyo, Japan) into a real-time monitoring system (Uchimura et al. 2010). Three moisture sensors were integrated and installed with tilt sensors units at sites No. 9, No. 10 and No. 12, respectively. The No. 12 moisture sensor was installed with a tensiometer for the reconstruction of the soil water retention curve (SWRC). A ground vibration detector was installed to capture the micro-ground shaking that was potentially induced by the bounce and tumble of landslide material against the underlying ground on April 24, 2016 (Fig. 3). The extreme humidity and temperature in the field challenged the functionality of these electronic sensors; however, most of the sensors

Fig. 2 The co-seismic landslide in the Yindongzi gulley that initiated and transformed into a debris flow by subsequent rain storms after the 2008 Wenchuan earthquake on August 13, 2009 (**a**), July 17, 2010 (**b**) and July 9, 2013(**c**)

Fig. 3 Photographs of instruments used for landslide real-time monitoring and the early warning system. Soil moisture sensor (**a**) and tensiometer (**b**) data were integrated with data collected with Kantaro tilt sensors (**c**) and installed at the head of the slope in a hollow. (**d**) A tipping bucket rain gauge was connected to the data logger
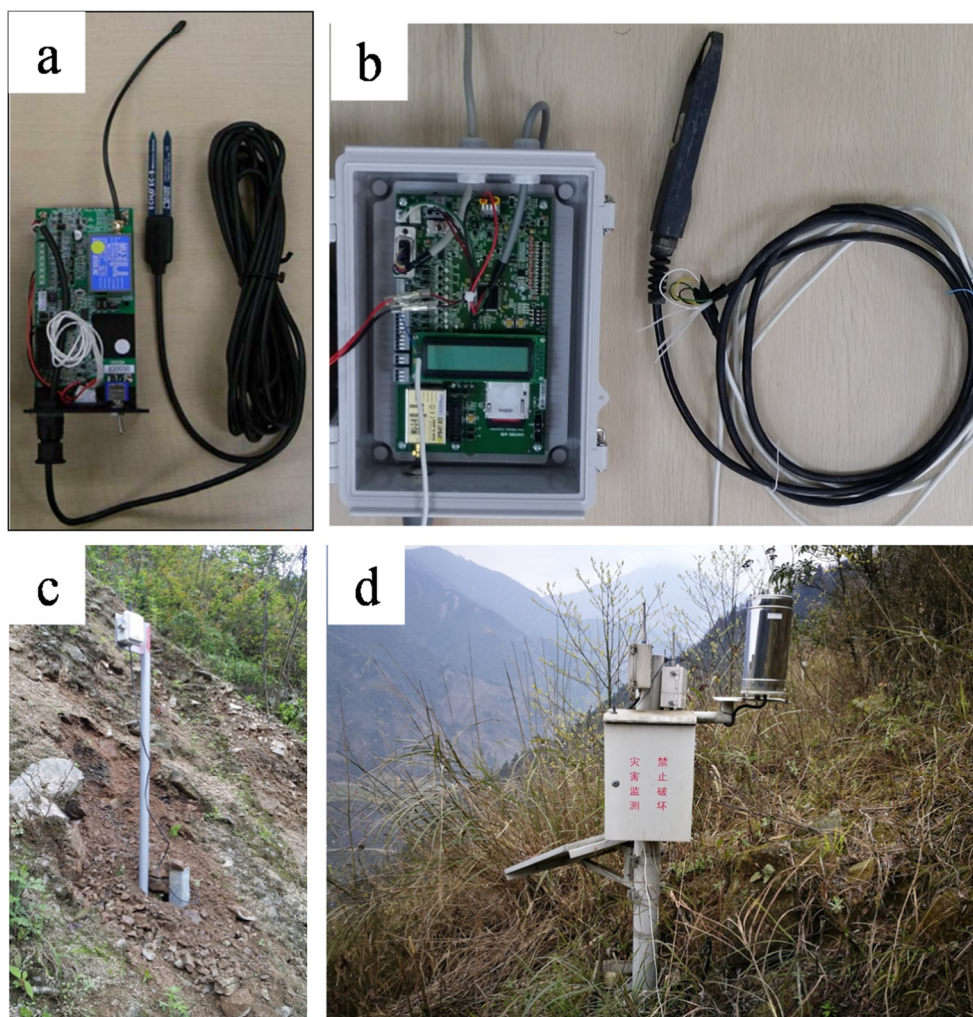
worked well when provided with periodic maintenance. The monitoring system collected real-time data and long-term variations in precipitation and soil moisture at the landslide from May 21, 2014 through to October 9, 2016. However, the tilt sensor did not incur any positive deformation during the monitoring period; therefore, changes were not observed in the inclinations other than some noise. Consequently, the displacement of the slope is not discussed or illustrated in this article.

Models for unsaturated soil stability analysis

In the current investigation we first analysed data observed from monitoring sites to measure changes in unsaturated hydrology and then we used these data to simulate the stress state and slope stability as modified by rainfall infiltration.

The SWRC is a function of the pressure head and can be calculated using the Brooks–Corey equations (Brooks and Corey 1964) as follows:

$$S_e(Z,t) = \frac{\theta(Z,t)-\theta_r}{\theta_s-\theta_r} = \begin{cases} |\alpha\psi(Z,t)|^{-n} &, \quad \alpha\psi < -1 \\ 1 &, \quad \alpha\psi > -1 \end{cases} \quad (1)$$

where θ_s is the saturated water content; θ_r is the residual water content; K_s is the saturated hydraulic conductivity; a, l and n are fitting parameters; S_e is the effective saturation, as defined as the equivalent degree of saturation, which is the ratio of free water volume to the total available volume (Lu et al. 2010).

A rainfall-induced shallow slope stability analysis under unsaturated conditions can be developed from classical slope stability methods by including the influence of suction stress on soil strength (Lu and Godt 2013). The unsaturated infinite-slope stability analysis is based on the safety factor approach that couples the Brooks–Corey equations and suction stress in unsaturated slopes. The suction stress can be calculated as a function of the soil moisture as follows:

$$\psi(Z,t) = \frac{S_e(Z,t)^{-\frac{1}{n}}}{\alpha} = \frac{\left(\frac{\theta(Z,t)-\theta_r}{\theta_s-\theta_r}\right)^{-\frac{1}{n}}}{\alpha} \quad (2)$$

$$\sigma^s(Z,t) = S_e\psi(Z,t) = \frac{\left(\frac{\theta(Z,t)-\theta_r}{\theta_s-\theta_r}\right)^{\frac{(n-1)}{n}}}{\alpha} \quad (3)$$

The suction stress $\sigma^s(Z, t)$ can also be calculated as a function of the pressure head as follows:

$$\sigma^s(Z, t) = \frac{|\psi(Z, t)|^{1-n}}{\alpha^n} \tag{4}$$

where σ^s is the suction stress, and ψ is the matric suction.

The safety factor of unsaturated slopes under transient infiltration conditions at depth Z below the ground surface at time t is given by the following equation (Baum et al. 2010; Lu and Godt 2013):

$$Fs(Z, t) = \frac{\tan\phi'}{\tan\beta} + \frac{c' - \sigma^s(Z, t)\tan\phi'}{(\gamma_d + \gamma_w \cdot \theta(Z, t))Z\sin\beta\cos\beta} \tag{5}$$

where ϕ' is the angle of internal friction for effective stress, c' is the soil cohesion for effective stress, γ_d is the dry soil unit weight, γ_w is the water unit weight, β is the slope angle and Z is the depth of the soil.

Results and discussion

Rainfall thresholds

The general method for estimating the critical rainfall threshold is based on the statistical analysis of data sets that include historical rainfall and disaster events. The daily precipitation during the monitoring period is plotted in Fig. 4. Observed daily rainfall was remarkably seasonal, and most of the rainfall events occurred during the rainy season, that is, from May to September. In particular, daily rainfall exceeding 100 mm was detected only once—on August 4, 2015. The maximum daily rainfall was only 113 mm in the region of the landslide in Yindongzi gully during the monitored rainy season, indicating that the frequency of severe storm rainfall was below average. Landslides or debris flows have not been triggered in the study

area since 2014, which increased the difficulty of linking the monitored rainfall and landslide events. Data on 14 landslide (debris flows) events and daily rainfall in the Yindongzi gully from 2009 to 2013 were collected from reports compiled by the relevant authorities and field interviews.

Owing to a lack of knowledge on the mechanisms of landslides, the statistical rainfall threshold retained uncertainties; therefore, a method to provide both rainfall thresholds and probabilities to express the uncertainties is more applicable in decision-making processes, especially for a site-specific landslide. Table 1 shows that the daily rainfall intensity for triggering landslides ranged from 39 to 217 mm and averaged 102.3 mm. All of the landslides had occurred during July and August, before 2014. The probability of a landslide event is determined based on the ratio of landslide events to rainfall events recorded within each category of rainfall amount, and the threshold is defined as the corresponding minimum triggering rainfall amount in each category. For example, Table 2 shows that nine reported landslide events were triggered among a total of 11 severe storm rainfall events that exceeded a threshold of 100.4 mm per day from 2009 to 2013 (accounting for a ratio of 81.82%). In other words, the probability of landslide occurrence under the condition of a severe rainstorm with a threshold of 100.4 mm is 81.82%, whereas the probability of a landslide under the condition of a heavy rainfall and rainstorm is 19.05% and 25%, respectively, and the corresponding rainfall threshold for each of these categories is 39 and 65.1 mm, respectively. Consequently, a rainfall *I-P* threshold model of landslide occurrence probability under rainfall conditions can be proposed as a linear function of the daily rainfall intensity and landslide probability (Eq. 6) using the statistics shown in Table 2.

$$P = 0.0077^*I_{24} - 0.0787 (10 \leq I_{24} \leq 140) \tag{6}$$

where P is the probability of landslide occurrence under the rainfall condition, and I_{24} is the daily rainfall intensity (mm).
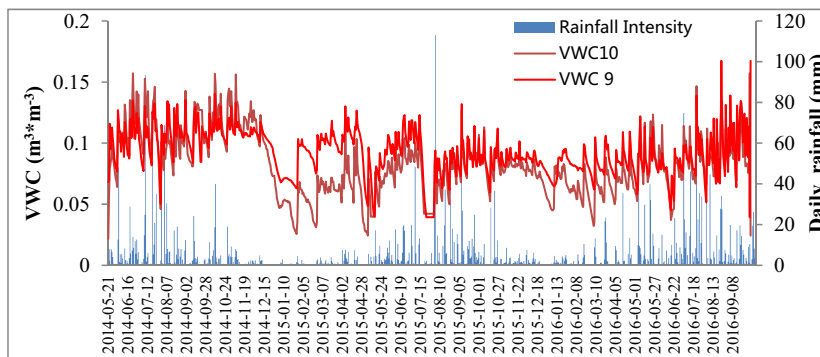

Fig. 4 Daily rainfall was recorded by the rain gauge at the monitored landslide area from May 21, 2014 to October 9, 2016. Instruments were installed on May 3, 2014, and data collection began on May 19, 2014. The volumetric water content (VWC) recorded by the soil moisture sensors (Decagon EC-5) at monitoring sites No. 9 and 10 at the landslide from May 21, 2014 to October 9, 2016 are represented by VWC 9 and VWC 10

Table 1 Daily rainfall that triggered landslide (debris flow) events in Yindongzi gulley, Dujiangyan County, from 2009 to 2013

Landslide event no.	Date (Y-M-D)	Daily rainfall (mm)
1	2009-7-17	100.40
2	2010-8-13	183.20
3	2010-8-19	101.00
4	2011-07-21	65.10
5	2011-08-15	42.00
6	2011-08-16	49.00
7	2011-08-21	144.80
8	2011-08-31	39.00
9	2012-08-18	105.60
10	2012-08-19	41.90
11	2013-07-08	111.60
12	2013-07-09	217.20
13	2013-07-26	108.80
14	2013-07-29	128.10

Y-M-D., Year-month-day

By neglecting the uncertainties raised from hydrological processes of rainfall infiltration, the *I-P* threshold model is expected to predict the extent of the probability and likelihood of rainfall-induced landslides under certain rainfall conditions and should be more applicable for decision-making processes and landslide hazard predictions, particularly for site-specific landslides. For example, compared with the estimated daily *I-D* threshold limit of 52 mm in the study area (Guo et al. 2016), eight rainfall events exceeding 52 mm and accounting for only 32% of the landslide probability predicted by the *I-P* model were recorded during the monitoring period; however, no debris flow was observed, which implies that a generalised rainfall threshold value may not always be applicable for forecasting site-specific landslides. Therefore, compared with the *I-P* threshold model, the *I-D* threshold provides only a minimum rainfall that could potentially trigger a landslide; however, it cannot consider the uncertainty and quantify the extent of the hazard when the rainfall intensity exceeds the threshold by a certain magnitude.

As mentioned above, the tilt data and results of the field investigation both indicated that obvious deformation and large-scale failure of the landslide and subsequent debris flows in the Yindongzi gully have not occurred since 2014, which implies that the activity leading to such hazards may have diminished in the Wenchuan earthquake region. This result is consistent with the findings of other studies (Yang et al. 2017), and the reasons can be summarised as follows. First, as previously stated, the rainfall intensity was below average in this region over the 3 study years. Second, the topsoil of landslides and deposits underwent a gradual consolidation and structural variations that affected the soil mechanisms. However, changes in rainfall thresholds and slope failure mechanisms with loose deposits during the post-earthquake period require further investigation.

Soil water retention curve

The SWRC of wide-gapped topsoil in the monitored landslide can be reconstructed based on the field measurements of matric suction and soil moisture during the rainy season. The tensiometer and soil moisture sensor (No. 12) were installed together to obtain the SWRC. Figure 4 shows that soil wetness significantly fluctuated during the wetting and drying periods. Soil moisture in the natural slope was repeatedly affected by drying and wetting processes because of evaporation and infiltration. During the study period, the fluctuation in soil moisture in the topsoil ranged between approximately 0.03 and 0.17 $m^3\ m^{-3}$. The soil moisture significantly increased in response to rainfall infiltration, and it decreased due to the processes of evaporation and drainage. During the rainy season, soil moisture increased by 5–13% following rainfall.

Although instrumentation malfunctions occurred at 1 month after installation and resulted in the loss of matric suction data, some suction data were available from 5 May to 23 May, 2016. Notable changes in matric suction occurred after rainfall events that exceeded approximately 39 mm within 24 h during this period (Fig. 5). Soil moisture rapidly fluctuated by an additional 0.01–0.08 $m^3\ m^{-3}$, and a similar change in matric suction of 2–40 kPa in response to drying and wetting processes was also observed. Therefore, we were able to establish the SWRC based on the data collected by monitoring soil moisture and matric suction during this period. In addition, the main

Table 2 Probability statistics under certain rainfall pattern conditions according to landslide and rainfall events

Rainfall pattern	Daily rainfall (mm)	Rainfall threshold (mm)	Landslide event	Rainfall event	Probability (%)
No rain	0	–	0	62	0.00
Light rain	0-10	0	0	98	0.00
Moderate rain	10-25	10	0	20	0.00
Heavy rain	25-50	39	4	21	19.05
Rainstorm	50-100	65.1	1	4	25.00
Severe storm	Above 100	100.4	9	11	81.82

Fig. 5 Variations in volumetric water content, soil matric suction and daily precipitation observed from May 5 to May 23, 2016 in the monitored landslide
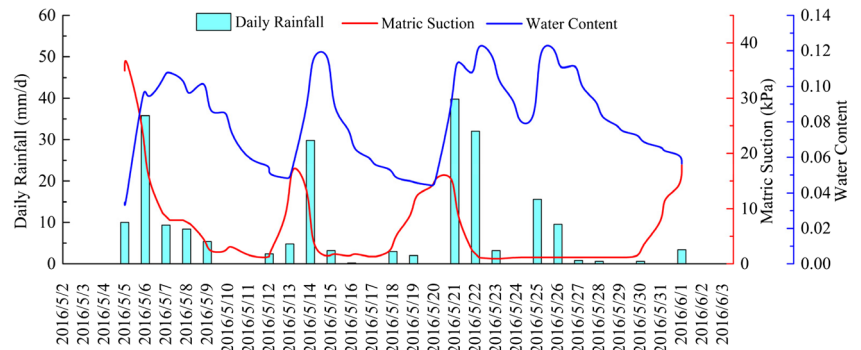
drying and wetting curves were determined in the fitting of the SWRCs to address adsorption and desorption paths.

Figure 6 shows the SWRC estimated in accordance with the Brooks–Corey (1964) model. Table 3 presents the results of estimating the parameters for unsaturated soil in the monitored landslide for both the wetting and drying processes. As shown in this table, the values of n are small, whereas the value of α is high, especially for the wetting process, since the topsoil primarily consists of gravel and features a smaller air-entry pressure due to the scarcity of fine particles and a wide-gapped grading texture. This finding is similar to that from a recent study of the SWRC of a wide-gapped gravelly loam from the landslide in the Wenchuan earthquake region (Yang et al. 2017) and is a reasonable result for seismic landslide deposits because the landslide material contains large amounts of fractures and macropores after an earthquake and the soil texture is relatively coarse. Therefore, the soil hydraulic and soil mechanic properties of the landslide material are unique compared with those of fine-texture soil (Cafaro 2002; Cafaro and Cotecchia 2015), and the hydraulic conductivity is relatively high. Figure 6 also demonstrates that the SWRC differs between drying and wetting processes, a phenomenon referred to as hysteresis. The SWRC exhibited a lower matric

suction during the wetting process than during the drying process at the same volumetric water content. The air-entry pressures ($1/\alpha$) for the wetting and drying processes were 0.09 and 1.2 kPa, respectively.

Hysteresis is generally caused by a tortuous soil pore structure and/or a difference in affinity between soil grains and water under different wetting regimes that is believed to affect the dynamics of water movement and stress distribution in unsaturated soil (Lu and Godt 2013). However, the matric suction detector, which is considered to be maintenance free when used to detect soil matric potential, failed in our study to monitor long-term data after the fitting period. It is therefore a challenging task to obtain long-term measurements of soil suction, especially for a soil of coarse texture. The limitations of the observed suction data imply that future research should include follow-up work to identify an alternative suction sensor and to evaluate whether the sensor is applicable for the long-term observation of gravel deposits. The SWRC also provides the fundamental functions and parameters for the subsequent hydro-mechanical analysis. Thus, a precise SWRC must be obtained via sophisticated approaches, which are urgently needed for the monitoring of unsaturated, wide-gapped, gravel landslides.
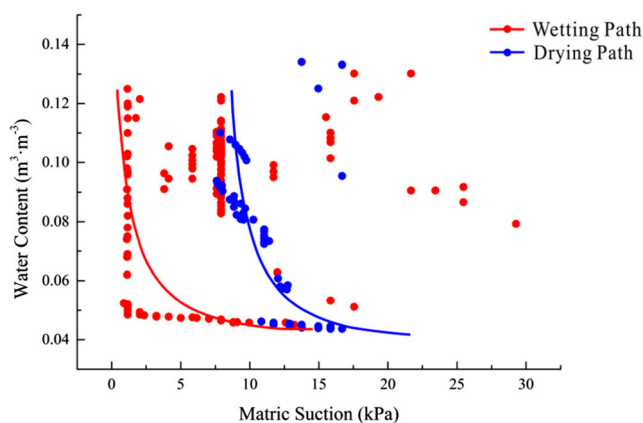

Fig. 6 Soil water characteristic curves (SWRC) during the analysed period in the top soil of the monitored landslide. The drying (desorption) curve (blue line) and wetting (adsorption) curve (red line) are shown (Colour figure online)

Table 3 Soil parameters for slope stability analysis

Symbol	Parameter	Value
c'	Soil cohesion for effective stress (kPa)	3.0
ϕ'	Angle of internal friction for effective stress (°)	33
γ_d	Dry soil unit weight;(kN/m^3)	15
β	Slope angle (°)	60
θ_r	Residual water content (−)	0.05
θ_s	Saturated water content (−)	0.45
Z	Soil depth (m)	0.5
aw	SWRC parameter for the wetting process	11
nw	SWRC parameter for the wetting process	0.53
ad	SWRC parameter for the drying process	0.83
nd	SWRC parameter for the drying process	0.73

SWRC, Soil water retention curve

Fig. 7 Variations in the modelled matric suction of the soil layer at the monitored landslide from May 21, 2014 to October 9, 2016. *WP, DP* Matric suction modelled by the SWRC parameters of the wetting process and drying process, respectively, as shown in Table 3
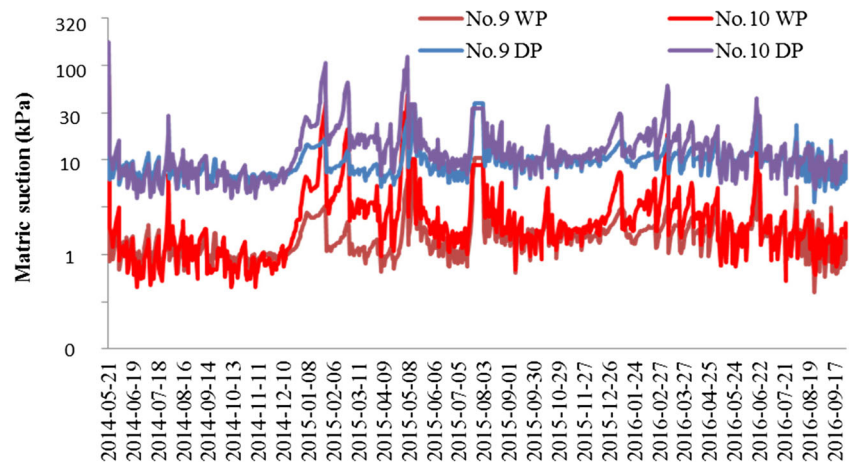
Suction stress

Suction stress describes the general state of soil stress in unsaturated slopes and is described as a function of the effective saturation and soil suction (Lu and Godt 2013). In this study, the parameters estimated from the SWRC were adopted to determine matric suction and suction stress in the unsaturated topsoil of the landslide area, and the effect of hysteresis was accounted for in these analyses.

Based on the soil moisture measured by the field instruments, the matric suction in the unsaturated soil layer was calculated by the Brooks–Corey method using the wetting and drying curve parameters. Figure 7 shows the variations in the matric suction of the soil layer at different monitoring points. The matric suction ranged from 0.39 to 79.81 kPa and from 3.55 to 124.14 kPa during the wetting and drying processes, respectively. Accordingly, suction stress exhibited a specific relationship with both effective saturation and matric suction. Based on Lu's model (2013), suction stress can be simulated by multiplying matric suction and effective saturation. Figure 8 presents the variations in suction stress based on the suction stress and topsoil soil moisture monitoring data. Suction stress ranged from 0.18 to 1.75 kPa and from 1.63 to 4.41 kPa in the wetting curve and drying curve, respectively (Fig. 6). The field capacity in the topsoil was relatively low

due to the coarse soil texture, and the effective saturation was relatively low during the monitoring period. Therefore, suction stress demonstrated a low value during the fluctuations. In general, the contribution of suction stress to the strength of the unsaturated slope is relatively small in magnitude; however, its contribution is substantial for the stability of the shallow topsoil on steep slopes at a depth of less than 1 m.

The difference in suction stress hysteresis ranges from approximately 1.45 to 2.66 kPa (Fig. 6), which is significant enough to determine the stability of a shallow slope with respect to rainfall infiltration. For a given soil moisture value, the corresponding suction stress presents a lower strength state along the wetting path than along the drying path. Thus, the hysteresis effect may largely influence the dynamics of unsaturated soil hydrology and, ultimately, the stress state of hillslopes.

Unsaturated slope stability analysis

The slope stability of shallow landslides under variably saturated conditions can be calculated using the infinite slope stability approach (Lu and Godt 2013). The depths and slope gradient of the geometry of landslides and slumps along the depression of the eroded gully are assumed to be 0.5 m and 60°, respectively, according to the field investigation. The

Fig. 8 Variations in the modelled suction stress of the soil layer at the monitored landslide from May 21, 2014 to October 9, 2016. *WP, DP* Suction stress modelled by the SWRC parameters of the wetting process and drying process, respectively, as shown in Table 3
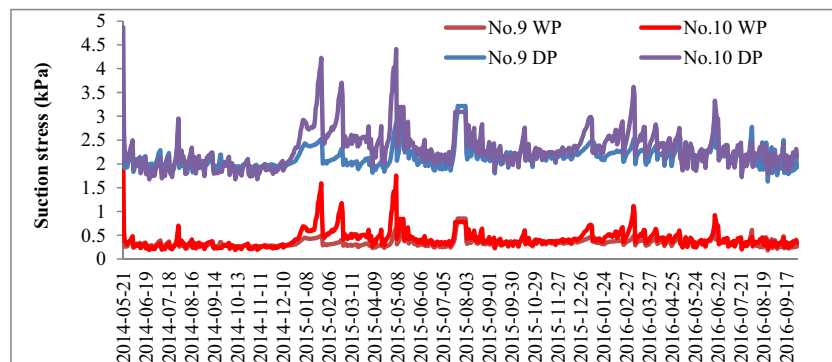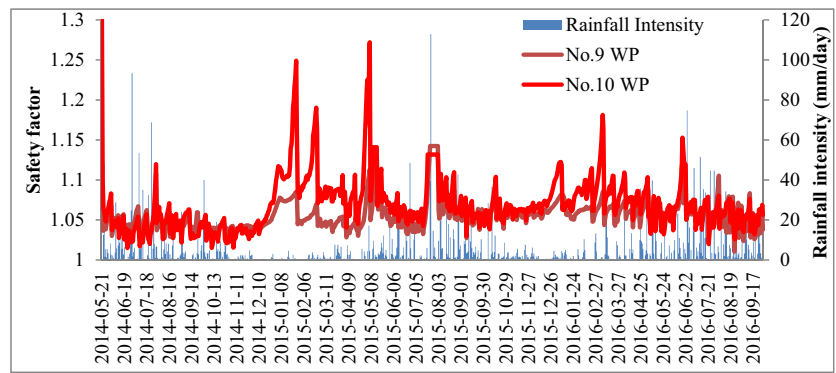
Fig. 9 Modelled safety factors based on variations in suction stress in monitored landslide from May 21, 2014 to October 9, 2016. *WP* safety factor modelled by the SWRC parameters of the wetting process

safety factor for quantifying slope stability was calculated using Eq. 5, which considered hydrological and soil mechanical conditions. For the slope stability analysis, the soil parameters of the topsoil of the slope are based on the SWRC, and its parameters are presented in Table 3.

The stability of an unsaturated slope is related to both the suction stress and the specific weight of the soil. Changes in soil specific weight and suction stress of landslide material were caused by soil moisture variations due to rainfall infiltration under unsaturated conditions. Soil suction stress significantly contributed to slope instability, especially for shallow landslides with relatively low effective cohesion values. Variations in soil moisture, matric suction and suction stress were used as inputs to calculate factor safety, with a safety factor below unity indicating slope failure. The effect of hysteresis was not accounted for in the slope stability analysis, and the safety factor of the slope was calculated based on the parameters of the wetting curve. Rainfall-induced landslides were associated with rainfall infiltration, and the wetting process was more relevant and radical with slope failures. Therefore, the SWRC of the wetting curve was considered in the slope stability analysis in this study.

The safety factor was determined, and the transient effects of infiltration on stability are shown in Fig. 9. The safety factor of the monitored landslide mainly ranged from 1.01 to 1.25 from May 2014 to October 2016.

Figure 9 shows the slope safety factor calculated to evaluate the stability of the corresponding natural slope, taking into consideration the suction stress of the unsaturated soil layer; the calculated value indicates that the safety factor fluctuated with infiltration of rainfall. In particular, the safety factor of the natural slope exhibited continuous fluctuations due to the changes in suction stress triggered by the evaporation and infiltration of water in the unsaturated soil layer. Correspondingly, the ground vibration detector observed some responses during the rainy seasons. Figure 10 shows that the ground vibration detector recorded 20, 17 and 33 responses (a total of 70 responses) from August 23 to 25, 2016 at precipitation levels of 28, 34 and 27 mm, respectively, for a total precipitation amount of 89 mm. The modelled safety factor decreased to its lowest value of 1.01 during this period. The massive number of ground vibration records must have been caused by miniature slope failures that occurred when the modelled safety factors came close to unity, which indicated a quasi-stable state of the slopes. However, the limitations of the ground vibration records should be mentioned. Certain ground vibration records did not show a univocal correlation with decreases in the safety factor because responses were detected when ground vibrations exceeded the acceleration threshold of 0.375 g. This result indicates that other sources of noise, such as human activities and earthquakes, could be excluded.

Fig. 10 Variations in ground vibration records and modelled safety factor during May 1 to August 30, 2016 in the monitored landslide
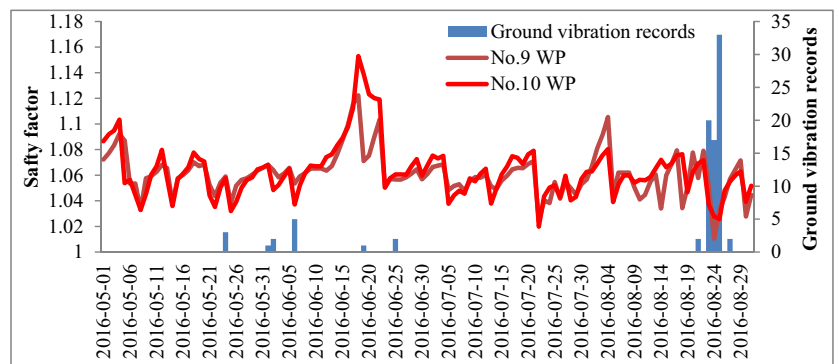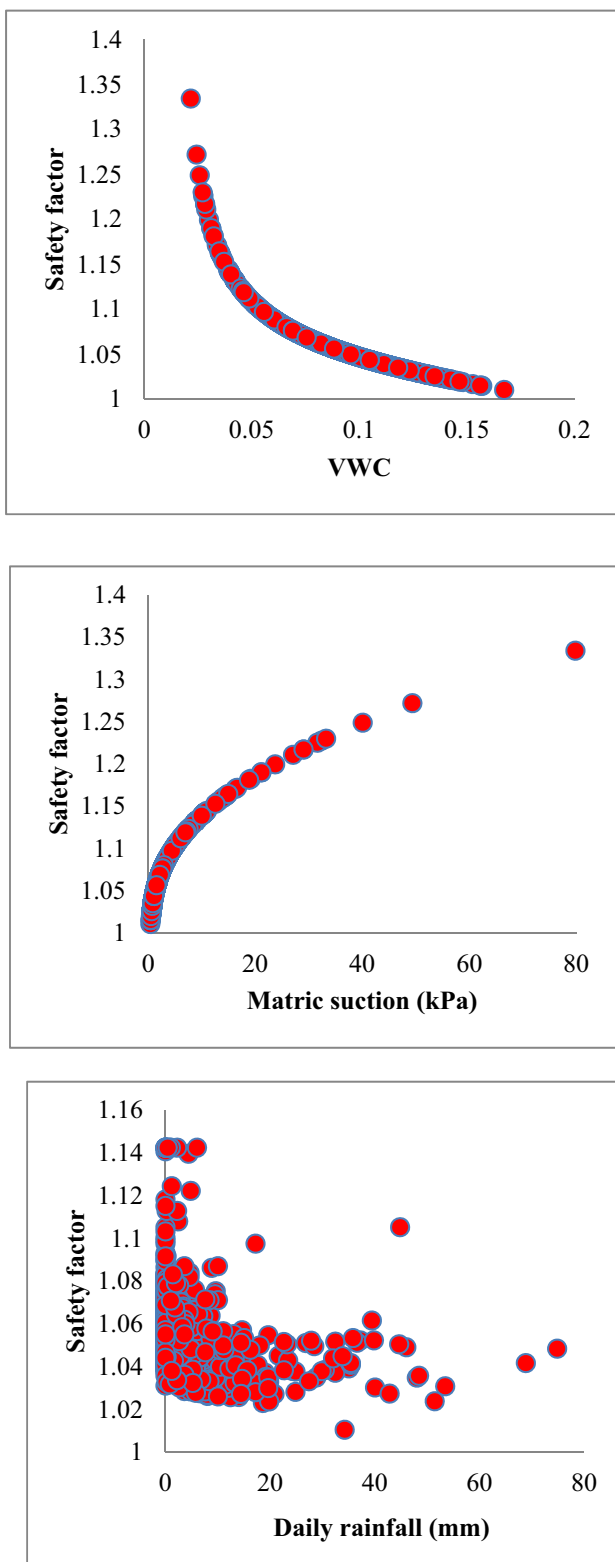
Fig. 11 Correlation of slope stability with volumetric water content, matric suction and daily rainfall plotting by stability analysis. Modelled safety factor versus observed VWC (**a**), modelled suction according to the SWRC model (**b**), observed daily rainfall (**c**), which indicates the soil moisture and matric suction thresholds for the rainfall-induced landslide early warning of the Wenchuan earthquake region

Hydrological thresholds

Through the use of in situ big data from observation studies and variably saturated slopes stability analysis in response to rainfall, an early warning system for rainfall-induced landslides in the Wenchuan earthquake region can be defined using the soil moisture and matric suction data as hydrological parameter criteria. This system can be established by comparing the safety factor with these criteria. Figure 11 illustrates the comparison of slope stability with soil moisture and matric suction and shows a strong correlation; the results imply that the critical values of volumetric soil moisture and matric suction for landslide initiation were approximately 0.16 m^3 m^{-3} and 2.0 kPa, respectively. Nevertheless, the correlation of the safety factor with the measured daily rainfall was relatively weak; this finding appears to be accurate because only water that infiltrated into the topsoil modified the stability of the slope. The hydrological process divided rainfall into infiltration, evaporation, retention and flow, which could lead to uncertainty in the statistical rainfall-based threshold. However, a rainfall-based threshold is still useful for long-term historical monitoring information on both landslide occurrences and triggering rainfall events. As a supplement to rainfall-based early warning strategies, implementing moisture content and suction threshold models based on slope failure mechanisms for the early warning of rainfall-induced landslides should improve the accuracy of shallow landslide and debris flow early warning systems in earthquake-prone regions.

The hydro-mechanical analysis-based method proposed here is used to identify multivariable thresholds for the early warning of rainfall-induced landslides. However, soil moisture and matric suction thresholds have been analytically identified using the SWRC; therefore, their reliability will depend on the goodness of fit of the SWRC (Cafaro 2002; Cafaro and Cotecchia 2015;Yang et al. 2017), which highlights the significance of an appropriate SWRC approach. The proposed thresholds should be verified and adjusted by observations in the field and future explorations of the soil–water mechanism. Moreover, due to the scarcity and specific positions of the tilt sensors installed in the landslide, variations in inclination were not observed during the analysed period. However, the correlation between inclination and hydrological parameters is important and worthy of further research.

Conclusion

The hydrological and mechanical characteristics of rainfall-induced landslides under variably saturated conditions provide insight into the mechanisms associated with the initiation of mountain hazards and are therefore significant benchmarks of rainfall-induced landslide early warning methods. In this study, long-term variations in hydrological processes of

landslide material were revealed, and a framework for identifying multivariate hydrological parameters for inclusion in an early warning system for landslides is proposed. These preliminary results demonstrate the feasibility of identifying multivariable thresholds by coupling in situ monitoring data and hydro-mechanical analyses. The following conclusions can be drawn from these analyses.

1) Daily rainfall intensity and landslide events were correlated, and then a model calculating the probability of landslides under certain rainfall conditions was proposed as an early warning criterion for rainfall-induced landslides. The proposed *I-P* threshold model is capable of predicting the likelihood of rainfall-induced landslides under certain rainfall conditions, and it should be applicable to decision-making processes and landslide risk predictions.

2) The observed SWRC parameters during the wetting and drying phases of the in situ monitoring period were expected as a reference for wide grades of unsaturated gravel mass. The comparison between wetting and drying processes demonstrated that hydro-mechanical hysteresis exists and is a dominant factor in the post-earthquake landslide remobilization under partially saturated hydrological conditions.

3) Long-term fluctuations in suction stress, matric suction and slope stability caused by rainfall infiltration were modelled. Corresponding slope failures were observed during a rainy period by the ground vibration detector, and the records indicated that the rise in moisture content and the fall in matric suction in response to rainfall infiltration have a great influence upon post-earthquake slope instability, especially in terms of shallow landslides.

4) Based on the coupling between instrumental field measurements and quantitative slope stability analysis under unsaturated conditions, a method for determining hydrological parameters, including matric suction, soil moisture and daily rainfall intensity, was proposed, which is expected to be applicable for use as multivariate criteria in an early warning system for post-earthquake landslides and debris flow.

Coupling unsaturated soil mechanics principles and in situ big data can provide insight into the initiation of rainfall-induced shallow landslides. Our results indicate that field measurements and threshold criteria, such as for pore pressure (soil suction), soil wetness and precipitation, provide significant data for distinguishing the stage of rainfall-induced slope stability evolvement. These measurements, combined with multivariate thresholds for forecasting landslide initiation, provide powerful tools that could be implemented in a landslide early warning system to reduce the risk of landslides.

References

Aleotti P (2004) A warning system for rainfall-induced shallow failures. Eng Geol 73:247–265. https://doi.org/10.1016/j.enggeo.2004.01.007

Baum RL, Godt JW, Savage WZ (2010) Estimating the timing and location of shallow rainfall-induced landslides using a model for transient, unsaturated infiltration. J Geophys Res 115:F03013. https://doi.org/10.1029/2009JF001321

Berti M, Simoni A (2010) Field evidence of pore pressure diffusion in clayey soils prone to landsliding. J Geophys Res Earth Surf 115(F3): F03031

Brooks RH, Corey AT (1964) Hydraulic properties of porous media. Colorado State University, Denver

Cafaro F (2002) Metastable states of silty clays during drying. Can Geotech J 39(4):992–999. https://doi.org/10.1139/t02-039

Cafaro F, Cotecchia F (2015) Influence of the mechanical properties of consolidated clays on their water retention curve. Italian Geotechnical Journal 2:13–29

Caine N (1980) The rainfall intensity–duration control of shallow landslides and debris flows. Geogr Ann A Phys Geogr 62:23–27

Chae B-G, Park H-J, Catani F, Simoni A, Berti M (2017) Landslide prediction, monitoring and early warning: a concise review of state-of-the-art. Geosci J 21(6):1033–1070. https://doi.org/10.1007/s12303-017-0034-4

Fan YB, Yang SW, Xu LK, Li SH, Feng C, Liang BF (2016) Real-time monitoring instrument designed for the deformation and sliding period of colluvial landslides. Bull Eng Geol Environ 76(3):829–838. https://doi.org/10.1007/s10064-016-0848-8

Godt JW, Baum RL, Lu N (2009) Landsliding in partially saturated materials. Geophys Res Lett 36. https://doi.org/10.1029/2008GL035996

Greco R, Comegna L, Damiano E, Guida A, Olivares L, Picarelli L (2013) Hydrological modelling of a slope covered with shallow pyroclastic deposits from field monitoring data. Hydrol Earth Syst Sci 17(10):4001–4013

Guo X, Cui P, Li Y, Ma L, Ge Y, Mahoney WB (2016) Intensity–duration threshold of rainfall-triggered debris flows in the Wenchuan earthquake affected area, China. Geomorphology 253:208–216. https://doi.org/10.1016/j.geomorph.2015.10.009

Guzzetti F, Peruccacci S, Rossi M, Stark C (2008) The rainfall intensity–duration control of shallow landslides and debris flows: an update. Landslides 5:3–17. https://doi.org/10.1007/s10346-007-0112-1

Lu N, Godt JW (2013) Hillslope hydrology and stability. Cambridge University Press, Cambridge

Lu N, Godt JW, Wu DT (2010) A closed-form equation for effective stress in unsaturated soil. Water Resour Res 46(5):111. https://doi.org/10.1029/2009wr008646

Ma F, Li Z, Wang J, Ding K (2016) Monitoring and engineering geology analysis of the Zhangmu landslide in Tibet, China. Bull Eng Geol Environ 76(3):855–873. https://doi.org/10.1007/s10064-016-0901-7

Palis E, Lebourg T, Tric E, Malet JP, Vidal M (2017) Long-term monitoring of a large deep-seated landslide (La Clapiere, south-east French alps): initial study. Landslides 14(1):155–170

Shao W, Bogaard TA, Bakker M, Berti M (2016) Analysing the influence of preferential flow on pressure propagation and landslide triggering of Rocca Pitigliana landslide. J Hydrol 543:360–372

Shao W, Ni J, Leung AK, Su Y, Ng CWW (2017) Analysis of plant root–induced preferential flow and pore–water pressure variation by a dual–permeability model. Can Geotech J 54:1537–1552

Sidle RC, Bogaard TA (2016) Dynamic earth system and ecological controls of rainfall-initiated landslides. Earth Sci Rev 159:275–291. https://doi.org/10.1016/j.earscirev.2016.05.013

Song YS, Chae BG, Lee J (2016) A method for evaluating the stability of an unsaturated slope in natural terrain during rainfall. Eng Geol 210:84–92. https://doi.org/10.1016/j.enggeo.2016.06.007

Tang C, Zhu J, Li WL, Liang JT (2009) Rainfall-triggered debris flows following the Wenchuan earthquake. Bull Eng Geol Environ 68:187–194. https://doi.org/10.1007/s10064-009-0201-6

Uchimura T, Towhata I, Anh TTL et al (2010) Simple monitoring method for precaution of landslides watching tilting and water contents on slopes surface. Landslides 7(3):351–357. https://doi.org/10.1007/s10346-009-0178-z

Wieczorek GE, Morgan BA, Campbell RH (2000) Debris-flow hazards in the blue ridge of central Vuginia. Environ Eng Geosci 6:3–23. https://doi.org/10.2113/gseegeosci.6.1.3

Xia M, Ren GM, Zhu SS, Ma XL (2014) Relationship between landslide stability and reservoir water level variation. Bull Eng Geol Environ 74(3):909–917. https://doi.org/10.1007/s10064-014-0654-0

Yang Z, Qiao J, Uchimura T, Wang L, Lei X, Huang D (2017) Unsaturated hydro-mechanical behaviour of rainfall-induced mass remobilization in post-earthquake landslides. Eng Geol 222:102–110. https://doi.org/10.1016/j.enggeo.2017.04.001